

Optimal operation of transition-edge sensors on ballistic membranes

T. Kühn and I. J. Maasilta

*Nanoscience Center, Department of Physics, University of Jyväskylä,
P.O. Box 35, FIN-40014 University of Jyväskylä, Finland*

(Dated: December 3, 2018)

We calculate the operating parameters of a transition edge sensor that is mounted on a thin dielectric membrane with the assumption that the phononic heat transport in the membrane is ballistic. Our treatment uses the correct phonon modes from elasticity theory (Lamb-modes), and spans the transition from 3D to 2D behavior. The phonon cooling power and conductance have a global minimum as function of membrane thickness, which leads to an optimal value for the membrane thickness with respect to noise equivalent power at a fixed operating temperature. The energy resolution of a calorimeter will not be affected strongly, but, somewhat counterintuitively, the effective time constant can be reduced by decreasing the membrane thickness in the 2D limit.

Superconducting transition edge sensors (TES) are currently under heavy development to be used as ultra-sensitive calorimeters and bolometers over a wide range of frequencies, from sub-mm radiation to gamma rays.¹ Some recent examples of ambitious projects using TES sensors are: the new sub-mm camera for the James Clerk Maxwell telescope (SCUBA-II)², the detection of single near-infrared photons for quantum cryptography³, the X-ray imaging spectrometers for future ESA, NASA and JAXA missions⁴, and the γ -ray detection of nuclear materials⁵. In most of these detector designs, the superconducting TES film has been thermally isolated from the surroundings by mounting it on a thin dielectric membrane, usually made of amorphous silicon nitride (SiN_x) due to ease of fabrication. This membrane limits the thermal conductance to the bath, and is therefore critical for the operation of the devices.

The phonon transport in the membrane can be either diffusive or ballistic, depending on how easily phonons are scattered in the sample. At the low temperatures where TESes are operated (~ 0.1 K), the bulk scattering mechanisms (mass impurities, phonon-phonon scattering, phonon-two-level system scattering) become very weak,⁶ leading to surface limited thermal conduction. If, in addition, the surfaces are smooth on the length scale of the dominant thermal phonons, the surface scattering is mostly specular, and phonon transport becomes ballistic.⁷ Ballistic phonon transport has been observed for crystalline bulk samples a long time ago⁸, but was also recently shown to be valid for some SiN_x membranes^{9,10}. For thermal sources such as TES film radiators in the ballistic limit, the analogy with photon thermal blackbody radiation is apparent if the substrate is three-dimensional. Then the emitted power has the typical Stefan-Boltzmann form $P = A\sigma T^4$, where for phonons $\sigma = \pi^5 k_B^4 / (15h^3) \sum e_i / c_i^2$, summing over the different phonon modes with speeds of sound c_i and radiator emissivities e_i .¹¹ On the other hand, it is less clear what happens to ballistic phonon transport when the substrate becomes two-dimensional. This is a realistic concern, as the dominant emitted phonon wavelength is of the order of $1\mu\text{m}$ for SiN at 100 mK,¹² comparable with a typical membrane thickness, so that many practical devices are

at least approaching the 2D limit.

In this paper, we describe a theory for operating TES detectors on thin membranes, spanning the transition from a fully 3D to a fully 2D substrate (membrane), using elasticity theory. The eigenmodes of a thin membrane are no longer the usual plane wave phonons, but are so called Lamb modes, with non-trivial displacement fields and dispersion relations.¹⁴ For this reason, thermal conduction¹⁵ and the phononic heat capacity¹⁶ are strongly affected, leading to the interesting effect that radiated power and thermal conductance have an absolute minimum as a function of the membrane thickness. Because of this effect, the noise equivalent power (NEP) also has a minimum, leading to the notion of an optimal membrane thickness for TES bolometers. However, the effective time constant also has a maximum at the same point, thus, one needs to make sure that the negative effect of slowing the detector down is not critical for the application. We also calculated the influence of thin membranes on the phonon noise limited energy resolution of TES calorimeters, and found that the effect is weak, especially around the optimal detector temperature.

In isotropic 3D bulk systems there are three independent phonon modes, two transversally and one longitudinally polarized, with sound velocities c_t and c_l , respectively. In the presence of boundaries, the bulk phonon modes couple to each other and form a new set of eigenmodes, which in the case of a free standing membrane are horizontal shear modes (h) and symmetric (s) and antisymmetric (a) Lamb modes¹⁴. The frequency ω for the h modes is simply $\omega = c_t \sqrt{k_{\parallel}^2 + (m\pi/d)^2}$, where k_{\parallel} is wave vector component parallel to membrane surfaces, d is the membrane thickness and the integer m is the branch number. However, the dispersion relations of the s and a Lamb modes cannot be given in a closed analytical form, but have to be calculated numerically.¹⁷ The lowest three branches, dominant for thin membranes at low temperatures, have low frequency analytical expressions:

$$\omega_{h,0} = c_t k_{\parallel} \quad (1a)$$

$$\omega_{s,0} = c_s k_{\parallel} \quad (1b)$$

$$\omega_{a,0} = \frac{\hbar}{2m^*} k_{\parallel}^2 \quad (1c)$$

where $c_s = 2c_t \sqrt{(c_l^2 - c_t^2)/c_l^2}$ is the effective sound velocity of the s mode, and $m^* = \hbar \left[2c_t d \sqrt{(c_l^2 - c_t^2)/3c_l^2} \right]^{-1}$ is an effective mass for the a -mode "particle". This lowest a -mode with its quadratic dispersion is mostly responsible for the non-trivial behavior for the detector performance described below.

To simplify the discussion, we assume that the thermal conductance is only limited by the membrane itself, in other words we do not consider the effects of electron-phonon non-equilibrium or thermal gradients within the TES film¹⁸, or of boundary resistance between the TES film and the membrane, and the membrane and the supporting 3D substrate. The importance of these added effects depends critically on the materials and detector geometry, and can in principle be minimized. With these assumptions the total heat flow out of the detector is

$$P = \frac{l}{2\pi^2} \sum_{\sigma,m} \int_0^{\infty} dk_{\parallel} k_{\parallel} \hbar \omega_{\sigma,m} \left| \frac{\partial \omega_{\sigma,m}}{\partial k_{\parallel}} \right| n(\omega, T), \quad (2)$$

where l is the circumference of the detector, $n(\omega, T)$ is the Bose-Einstein distribution and σ and m are the mode and branch indices.¹⁹ This expression can be used to compute the transition from 3D to 2D if enough branches are used. If the membrane is thin and temperature low, i.e. $Td \ll \hbar c_t/2k_B$, only the lowest branches (Eqs. 1) are occupied, and we are fully in the 2D limit, in which case

$$P_{2D} = \frac{l\hbar}{2\pi^2} \left[\left(\frac{1}{c_t} + \frac{1}{c_s} \right) \Gamma(3) \zeta(3) \left(\frac{k_B T}{\hbar} \right)^3 + \sqrt{\frac{2m^*}{\hbar}} \Gamma\left(\frac{5}{2}\right) \zeta\left(\frac{5}{2}\right) \left(\frac{k_B T}{\hbar} \right)^{5/2} \right]. \quad (3)$$

Note that the effective mass of the lowest a mode depends on the membrane thickness and hence in the 2D limit $P \propto 1/\sqrt{d}$. In the 3D limit $Td \gg \hbar c_t/2k_B$, the dominant phonon wavelength is much smaller than d , leading to decoupling of the longitudinal and transversal modes and

$$P_{3D} = \frac{\pi^2 l d \hbar}{120} \left(\frac{2}{c_t^2} + \frac{1}{c_l^2} \right) \left(\frac{k_B T}{\hbar} \right)^4. \quad (4)$$

As expected, $P_{3D} \propto d$. This means that decreasing the membrane thickness at a fixed temperature, the radiated power will first decrease with d , then reach a global minimum and will increase again, if we decrease d further. The minimum is approximately at the 2D-3D crossover thickness $d_C \equiv \hbar c_t/(2k_B T)$. The same behavior occurs for the differential thermal conductance $g = dP/dT$. In the 2D-3D crossover range, we have computed P and g

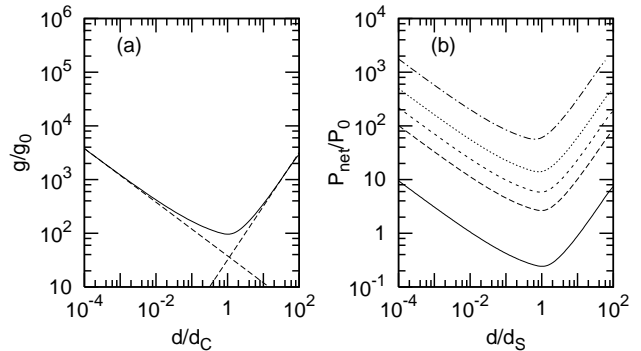


FIG. 1: (a) The differential thermal conductance g of a ballistic radiator as function of the membrane thickness d . The crossover thickness $d_C = \hbar c_t/2k_B T$. g is normalized with $g_0 = (k_B l c_t/8\pi^2)(k_B T/\hbar c_t)^2$. The asymptotic 2D and 3D limits, computed from Eqs. 3 and 4 are indicated by the dashed lines. (b) The net emitted power P_{net} of a detector at temperature T_D connected to the substrate at temperature T_S as function of membrane thickness d , for temperature ratios $T_D/T_S = 1.01, 1.1, 1.2, 1.4$ and 2.0 . Curves with higher T_D/T_S lie above curves with lower T_D/T_S . $d_S = \hbar c_t/2k_B T_S$ and $P_0 = l(k_B T_S)^3/(2\pi \hbar^2 c_t)$.

numerically, using the lowest 100 branches. Fig. 1(a), we plot g as a function of d , showing an increase of g by \sim factor of 5 when decreasing d from d_C to $10^{-2}d_C$, corresponding to changing d from 240 nm to 2.4 nm at 100 mK for SiN_x .

The net phonon cooling power of the detector is the difference between the power flow out of the detector and the power flow into the detector that is emitted from the substrate. Hence, if we denote the detector temperature by T_D and the substrate temperature by T_S , the total cooling power is $P_{net} = P(T_D) - P(T_S)$. In Fig. 1(b) we plot P_{net} as function of d for different ratios T_D/T_S . As we have two different temperatures, we chose to normalize the membrane thickness with respect to T_S and define the quantity $d_S \equiv \hbar c_t/2k_B T_S$. The thickness dependence is the same as for g , and as one would expect, the radiated power increases with increasing T_D . The place of the minimum is slightly shifted from curve to curve, as the 2D-3D crossover is dominated by the detector phonons at high T_D/T_S .

A useful way to operate TES detectors is by voltage biasing. This leads to negative electrothermal feedback (ETF), which speeds up the detectors and improves their sensitivity and energy resolution¹. For TES on thin ballistic membranes, the basic operational theory applies, as long as one takes into account the correct formulas for P_{net} and g as discussed above. Especially interesting is the question: Will the non-trivial thickness dependence lead to observable effects for the important detector parameters such as the noise equivalent power NEP, effective time constant τ_{eff} and energy resolution ΔE ? In the following we discuss this issue, noting that we only

consider here the contributions from the thermodynamic noise generated by the phonon thermal transport in the membrane, the so called phonon noise. Other noise mechanisms can be easily added to the discussion using known formulas¹.

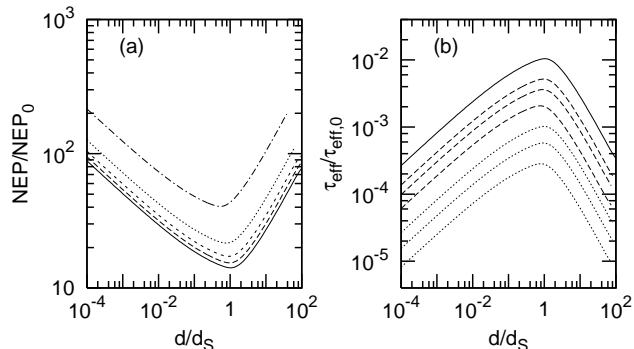


FIG. 2: (a) The ballistic phonon NEP of a TES as function of d for temperature ratios $T_D/T_S = 1.0, 1.1, 1.2, 1.4$ and 2.0 , ordered from bottom to top. The normalization constant is $\text{NEP}_0 = \sqrt{l/c_t(k_B T_S)^2/(2\pi\hbar)}$. (b) The effective time constant τ_{eff} as function of d for the same ratios $T_D/T_S = 1$ (solid line) and $1.1, 1.2$ and 1.5 for $\alpha = 10$ (dashed lines) and $\alpha = 100$ (dotted lines). Curves with higher T_D/T_S below curves with lower T_D/T_S for the same value of α . $\tau_{\text{eff},0} = 8\pi^2 \hbar^2 c_t \gamma V_{\text{el}} / (l k_B^3 T_S)$.

The phonon noise power spectral density for ballistic transport can be calculated from microscopic considerations,^{20,21} leading to an equation for the phonon NEP:

$$\text{NEP} = \sqrt{2k_B [T_D^2 g(T_D) + T_S^2 g(T_S)]}. \quad (5)$$

In Fig. 2(a), we plot the NEP as a function of d . It has a clear minimum, just like g , as expected from the simplicity of Eq. (5). In the 3D limit the NEP becomes proportional to \sqrt{d} , whereas in the 2D limit it approaches $d^{-1/4}$. The absolute minimum in the NEP means that it is possible to define the optimal membrane thickness d_{opt} , which gives the highest sensitivity for a TES bolometer at fixed T_D and T_S . For an equilibrium bolometer ($T_D = T_S$) $d_{\text{opt}} \approx d_S$, whereas for $T_D > T_S$, $d_{\text{opt}} \approx \hbar c_t / (2k_B T_D)$. For SiN_x membranes and $T_D = T_S = 0.1\text{K}$, $d_{\text{opt}} = 240$ nm.

In addition to sensitivity, an important characteristic of a bolometer is its response time τ_{eff} . For a voltage biased TES of volume V with its electronic heat capacity $C_{\text{el}} = \gamma V T_D$ being dominant, in the perfect voltage bias and low inductance limit¹ it is given by $\tau_{\text{eff}} = C_{\text{el}} / (g(T_D) + \alpha P_{\text{net}} / T_D)$, where $\alpha = T / R d R / d T$ is the steepness parameter of the transition under bias. Fig. 2(b) presents τ_{eff} as function of d for several values of T_D/T_S and two examples of $\alpha = 10, 100$. Now τ_{eff} has a maximum around $\hbar c_t / (2k_B T_D)$ and is proportional to \sqrt{d} in the 2D limit and to $1/d$ in the 3D limit.

Thus, if one wants to operate near d_{opt} , limitations of the time constant need to be considered. Fortunately, biasing strongly into the ETF (high α), helps to reduce τ_{eff} significantly.

In Fig. 3(a), we show the NEP as function of T_D for different values of d . In general the NEP increases with T_D . For a fixed value of T_D/T_S we can always find two membrane thicknesses that yield the same NEP, one with $d < d_S$ and one with $d > d_S$. However, the T_D dependence of these two values are quite different, as can be seen by comparing the slopes of the curves at crossing points.

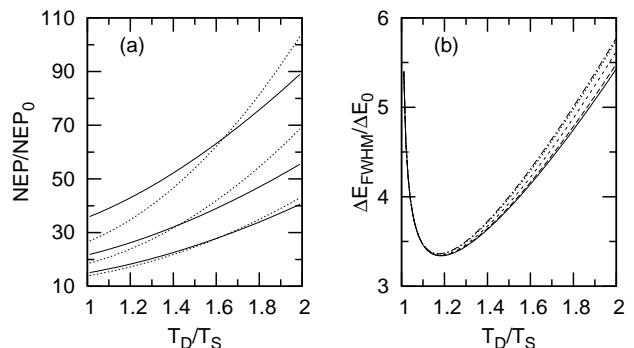


FIG. 3: (a) The phonon NEP vs. T_D/T_S for membrane thicknesses $d/d_S = 0.004, 0.04, 0.4, 1, 4$ and 40 . The curves for $d/d_S < 1$ are plotted with solid lines with higher curves corresponding to lower d , while dotted lines represent curves with $d/d_S \geq 1$ with lower curves corresponding to lower d . (b) The high \mathcal{L} FWHM energy resolution ΔE_{FWHM} of a TES as function of the ratio T_D/T_S for the membrane thicknesses $d/d_S = 0.04, 0.4, 1, 4$ and 40 , ordered from the bottom to the top. $\Delta E_0 = 2.8 \sqrt{\gamma V k_B T_S^3 / \alpha_I}$.

Finally, the phonon noise limited full width half maximum (FWHM) energy resolution of an optimally filtered TES calorimeter¹ for high loop gain $\mathcal{L} = \alpha P_{\text{net}} / (g(T_D) T_D) \gg 1$ is

$$\Delta E_{\text{FWHM}} = 2.355 \sqrt{k_B T_D^2 C_{\text{el}}} \frac{2}{\sqrt{\alpha_I}} \left(\frac{\text{NEP}^2}{4k_B T_D P_{\text{net}}} \right)^{1/4}, \quad (6)$$

where $\alpha_I = T / R d R / d T$. ΔE_{FWHM} is plotted as a function of T_D in Fig. 3(b) for different membrane thicknesses. It has a minimum just below $T_D/T_S \approx 1.2$, almost independent of d and in agreement with the 3D ballistic result²², so that an optimal T_D for a fixed T_S can be defined. For higher ratios T_D/T_S , the thinner membranes decrease ΔE_{FWHM} slightly, by about 6 % at $T_D/T_S = 2$ from $d = 40d_S$ to $d = 0.04d_S$.

Discussions with D.-V. Anghel and M. Manninen are acknowledged. This work was supported by ESA ESTEC contract no. 16759/02/NL/PA, the Academy of Finland project No. 118665 and EU project No. 505457-1.

-
- ¹ D. McCammon, in *Cryogenic Particle Detection*, edited by Ch. Enss (Springer, Berlin, 2005); K. Irwin and G. Hilton, *ibid.*
- ² W. Holland *et al.*, Proc. SPIE **6275**, 62751E (2006).
- ³ D. Rosenberg, S. W. Nam, P. A. Hiskett, C. G. Peterson, R. J. Hughes, J. E. Nordholt, A. E. Lita, and A. J. Miller, Appl. Phys. Lett. **88**, 021108 (2006).
- ⁴ <http://www.rssd.esa.int/XEUS>,
<http://constellation-x.gsfc.nasa.gov>,
<http://www.astro.isas.jaxa.jp/future/NeXT>
- ⁵ B. L. Zink, J. N. Ullom, J. A. Beall, K. D. Irwin, W. B. Doriese, W. D. Duncan, L. Ferreira, G. C. Hilton, R. D. Horansky, C. D. Reintsema, and L. R. Vale, Appl. Phys. Lett. **89**, 124101 (2006).
- ⁶ R. Berman, *Thermal Conduction in Solids*, (Clarendon Press, Oxford, 1976).
- ⁷ J. M. Ziman, *Electrons and Phonons*, (Oxford University Press, Oxford 1960), pp. 451-465.
- ⁸ R. J. von Gutfeld and A. H. Nethercot, Phys. Rev. Lett. **12**, 641 (1964).
- ⁹ W. Holmes, J. M. Gildemeister, P. L. Richards, and V. Kotsubo, Appl. Phys. Lett. **72**, 2250 (1998).
- ¹⁰ H. F. C. Hoevers, M. L. Ridder, A. Germeau, M. P. Bruijn, P. A. J. de Korte and R. J. Wiegerink, Appl. Phys. Lett. **86**, 251903 (2005).
- ¹¹ J. P. Wolfe, *Imaging Phonons*, (Cambridge University Press, Cambridge 1998), pp. 80-88.
- ¹² The transversal and longitudinal sound velocities for low-stress SiN_x are $c_t = 6200$ m/s and $c_l = 10300$ m/s, respectively¹³, giving dominant wavelengths $\lambda = hc_i/(2.82k_B T)$ as $\lambda_t = 1.0\mu\text{m}$ and $\lambda_l = 1.8\mu\text{m}$ at 0.1 K.
- ¹³ S. Wenzel, Ph.D. thesis, University of California at Berkeley, 1992.
- ¹⁴ B. A. Auld, *Acoustic Fields and Waves in Solids, volume II*, second edition, (Robert E. Krieger publishing company, Malabar 1990).
- ¹⁵ T. Kühn and I. J. Maasilta, Nucl. Instrum. Methods Phys. Res. A **559**, 724 (2006).
- ¹⁶ O. V. Fefelov, J. Bergli, and Y. M. Galperin, e-print cond-mat/0612462.
- ¹⁷ T. Kühn, D. V. Anghel, J. P. Pekola, M. Manninen and Y. M. Galperin, Phys. Rev. B **70**, 125425 (2004).
- ¹⁸ J. T. Karvonen, L. J. Taskinen and I. J. Maasilta, J. Low Temp. Phys. **146**, 213 (2007).
- ¹⁹ Note that the prefactor is $\frac{l}{2\pi^2}$ instead of the factor $\frac{l}{8\pi}$ that was mistakenly given in Ref. [15].
- ²⁰ W. S. Boyle and K. F. Rogers Jr., J. Opt. Soc. Am. **49**, 66 (1959).
- ²¹ The calculation in Ref. [20] assumed Poissonian phonon statistics. Eq. (5) is obtained for the correct quantum statistics, including the slightly superpoissonian nature of black-body radiation, I. J. Maasilta, unpublished.
- ²² I. J. Maasilta, Nucl. Instrum. Methods Phys. Res. A **559**, 706 (2006).